Institut de Recerca en Economia Aplicada Regional i Pública
Research Institute of Applied Economics

Document de Treball 2018/18 1/42 pág.
Working Paper 2018/18 1/42 pág.

"Time connectedness of fear"

Andrada-Félix J, Fernandez-Perez A, Fernández-Rodríguez F & Sosvilla-Rivero S

UB IREA
Institut de Recerca en Economia Aplicada | *Research Institute of Applied Economics*

Institut de Recerca en Economia Aplicada Regional i Pública
Research Institute of Applied Economics
Universitat de Barcelona
Av. Diagonal, 690 • 08034 Barcelona

WEBSITE: www.ub.edu/irea/ • CONTACT: irea@ub.edu

The Research Institute of Applied Economics (IREA) in Barcelona was founded in 2005, as a research institute in applied economics. Three consolidated research groups make up the institute: AQR, RISK and GiM, and a large number of members are involved in the Institute. IREA focuses on four priority lines of investigation: (i) the quantitative study of regional and urban economic activity and analysis of regional and local economic policies, (ii) study of public economic activity in markets, particularly in the fields of empirical evaluation of privatization, the regulation and competition in the markets of public services using state of industrial economy, (iii) risk analysis in finance and insurance, and (iv) the development of micro and macro econometrics applied for the analysis of economic activity, particularly for quantitative evaluation of public policies.

Abstract

This paper examines the interconnection between four implied volatility indices representative of the investors' consensus view of expected stock market volatility at different maturities during the period January 3, 2011-May 4, 2018. To this end, we first perform a static analysis to measure the total volatility connectedness in the entire period using a framework proposed by Diebold and Yilmaz (2014). Second, we apply a dynamic analysis to evaluate both the net directional connectedness for each market using the TVP-VAR connectedness approach developed by Antonakakis and Gabauer (2017). Our results suggest that a 72.27%, of the total variance of the forecast errors is explained by shocks across the examined investor time horizons, indicating that the remainder 27.73% of the variation is due to idiosyncratic shocks. Furthermore, we find that volatility connectedness varies over time, with a surge during periods of increasing economic and financial instability. Finally, we also document a superior performance of the TVP-VAR approach to connectedness respect to the original one proposed by Diebold and Yilmaz (2014).

JEL classification: C53, E44, F31, G15

Keywords: Implied volatility indices, Financial market Linkages, Connectedness, Vector Autoregression, Variance Decomposition.

Julián Andrada-Félixa: Department of Quantitative Methods in Economics, Universidad de Las Palmas de Gran Canaria, Las Palmas de Gran Canaria, Spain. E-mail: julian.andrada@ulpgc.es

Adrian Fernandez-Perez: Department of Finance, Auckland University of Technology, Auckland, New Zealand. E-mail: adrian.fernandez@aut.ac.nz

Fernando Fernández-Rodríguez: Department of Quantitative Methods in Economics, Universidad de Las Palmas de Gran Canaria, Las Palmas de Gran Canaria, Spain. E-mail: ffernandez@dmc.ulpgc.es

Simón Sosvilla-Rivero: Complutense Institute for International Studies, Universidad Complutense de Madrid. Madrid, Spain. E-mail: sosvilla@ccee.ucm.es

Acknowledgements

We thank Gary Koop and Dimitris Korobilis for providing the TVP-VAR programs.

Funding

This paper is based on work supported by the Spanish Ministry of Economy and Competitiveness [grant ECO2016-76203-C2-2-P].

1. Introduction

Volatility is a crucial ingredient in many different areas of macroeconomics (e.g., business cycle fluctuations or monetary policy transmission; Bloom *et al*., 2018, and Mankiw and Reis, 2002) and finance (e.g., asset allocation, option pricing, risk management or systemic risk measurement; Campbell, 2000), as well as a key factor influencing the effect of public information signals (Morris and Shin, 2002). High volatility may also anticipate a financial crisis as it is a signal of growing uncertainty (see, e. g., Baker *et al*., 2016, and Engle *et al*., 2013). Furthermore, investment risk varies not only with asset class, but also with investment horizon, thus creating a "term structure of the risk–return trade-off" (Campbell and Viceira, 2005).

A common way of measuring volatility in financial markets is through the implied volatility obtained from financial derivatives. The best-known applications of this methodology are the market volatility indices developed by the Chicago Board Options Exchange (CBOE). Based on the theoretical papers of Demeterfi *et al.* (1999) and Carr and Madan (1998), CBOE obtains the implied volatility from options markets[1]. The forward-looking nature of option market data allows deriving economically-based and model-free conditional risk measures. Since they represent the expectations of the investors about the future realized volatility of the underlying assets for certain calendar days ahead, the implied volatilities are often referred to as the "fear gauge" of financial markets by market participants and media (Whaley, 2000).

Prior studies have provided support for the predictive ability of the Volatility Index (VIX, a measure of implied volatility of the Standard & Poor's 500 Index) with regard to stock return (see, e.g., Giot, 2005; Guo and Whitelaw, 2006; Banerjee *et al.*, 2007,

[1] For excellent primers on the VIX, see Whaley (2009) and Gonzalez-Perez (2015). Carr and Lee (2009) provide an exemplary history of the market for volatility derivatives and a survey of the relevant methodologies for pricing and hedging volatility derivatives products.

inter alia). Furthermore, the forward-looking characteristic of implied volatility indices make them have a superiority of the information content over historical volatility measures as it has been extensively documented in the literature (Jorion, 1995; Xu and Taylor, 1995; Christenssen and Prabhala, 1998: Fleming, 1998; Blair, Poon, and Taylor, 2001; and Jiang and Tian, 2005; among others).[2]

More recently, Jabłecki *et al.* (2014) find that volatility term structure calculated from implied volatility index futures (VIX index, hereafter) at different maturities shows a clear pattern of dependence on the current level of the VIX index. Lu and Zhu (2010), empirically examine variance term structure based on time series data from the CBOE VIX futures market. Using a principal component analysis they provide evidence that a third factor, based on the curvature, is statistically significant to capture variance term structure dynamics. Johnson (2017) follows the methodology used to compute the VIX to form the VIX term structure to estimate the implied volatility over the next one, two, three, six, nine, and twelve months. He finds that a single factor, the second principal component (slope), summarizes nearly all information about variance risk premia in the VIX term structure. Branger *et al*. (2017) study the volatility-of-volatility (VVIX) term structure, finding that the slope of the VVIX (defined as VVIX's second principal component) predicts excess returns of Standard & Poor's 500 Index and VIX straddles, incrementing the informational content of the VIX term structure and the variance risk premium.

Financial economists have argued the asset allocation may be significantly different across investment horizons (see, e.g., Christoffersen and Diebold, 2000 or Campbell and Viceira, 2005). Although one could expect that the shorter-term VIX indices should

[2] Poon and Granger (2003) concluded that the VIX is the best predictor of realized volatility, although it may be a biased one.

be below the longer-term VIX indices as investors need to be compensated for unknown future risk, simple observation of the interaction between VIX indicators at different time horizons reveals a non-constant and irregular relation between them. We assert that this evidence could suggest that they react differently and by different degrees of incremental changes to the same economic event.

Motivated by such considerations, the aim of this paper is to systematically examine the nature and intensity of the volatility connectedness among VIX indicators representative of market-based expectations of volatility at different time horizons. We employ the shock connectedness measurement framework popularized by Diebold and Yilmaz (2012, 2014). This empirical framework, based on a generalized vector autoregressive (VAR) system, enables us to effectively quantify total (non-directional) connectedness, gross directional spillovers, net directional connectedness, and net pairwise connectedness. In particular, we perform a full-sample (static) analysis uncovering average or unconditional connectedness. Moreover, we employ the extension of the time-varying parameter VAR (TVP-VAR, hereafter) connectedness approach of Antonakakis and Gabauer (2017) to characterize dynamic connectedness.

The rest of the paper is organized as follows. Section 2 outlines the econometric framework to quantify both the total and directional volatility connectedness. Section 3 presents our data and a preliminary analysis. In Section 4, we report the empirical results (both static and dynamic) obtained for our sample of four market volatility indices (a system-wide measure of connectedness). Section 5 examines the evolution of net directional and net pairwise directional connectedness in each market. Section 6 provides robustness check. Finally, Section 7 summarizes the findings and offers some concluding remarks.

2. Methodology

The main tool for measuring the amount of connectedness is based on a decomposition of the forecast error variance. In this paper, we make use of Diebold and Yilmaz's connectedness methodology which we will briefly describe in Section 2.1. Finally, we also employ the dynamic connectedness based on TVP-VAR provided by Antonakakis and Gabauer (2017) which will be developed in Section 2.2.

2.1 Diebold and Yilmaz's (DY) connectedness.

Given a multivariate empirical time series, the forecast error variance decomposition is obtained from the following steps:

1. Fit a reduced-form vector autoregressive (VAR) model to the series,

$$Y_t = \beta Y_{t-1} + \varepsilon_t, \quad \varepsilon_t \sim N(0, \Sigma) \tag{1}$$

where Y_t, represents an *Nx1* series vector at time *t*, β is an NxN_p dimensional coefficient matrix and ε_t is an *Nx1* dimensional error disturbance vector with an *NxN* variance-covariance matrix, Σ.

2. Using series data up to and including time *t*, establish an *H* period-ahead forecast (up to time *t* + *H*).

3. Decompose the error variance of the forecast for each component with respect to shocks from the same or other components at time *t*.

Diebold and Yilmaz (2014) propose several connectedness measures built from pieces of variance decompositions in which the forecast error variance of variable *i* is decomposed into parts attributed to the various variables in the system. This section provides a summary of their connectedness index methodology.

Let us denote by d_{ij}^H the *ij*-th *H*-step variance decomposition component (i.e., the fraction of variable *i*'s *H*-step forecast error variance due to shocks in variable *j*). The connectedness measures are based on the "non-own", or "cross", variance decompositions, d_{ij}^H , $i, j = 1,\ldots,N, i \neq j.$

Consider an *N*-dimensional covariance-stationary data-generating process (DGP) with orthogonal shocks: $x_t = \Theta(L)u_t$, $\Theta(L) = \Theta_0 + \Theta_1 L + \Theta_2 L^2 + ...$, $E(u_t, u_t') = I.$ Note that Θ_0 need not be diagonal. All aspects of connectedness are contained in this very general representation. Contemporaneous aspects of connectedness are summarized in Θ_0 and dynamic aspects in $\{\Theta_1, \Theta_2, ...\}$. Transformation of $\{\Theta_1, \Theta_2, ...\}$ via variance decompositions is needed to reveal and compactly summarize connectedness. Diebold and Yilmaz (2014) propose a connectedness table such as Table 1 to understand the various connectedness measures and their relationships. Its main upper-left *NxN* block, which contains the variance decompositions, is called the "variance decomposition matrix," and is denoted by $D^H = [d_{ij}^H]$. The connectedness table increases D^H with a rightmost column containing row sums, a bottom row containing column sums, and a bottom-right element containing the grand average, in all cases for $i \neq j.$

[Insert Table 1 here]

The off-diagonal entries of D^H are the parts of the *N* forecast-error variance decompositions of relevance from a connectedness perspective. In particular, the *gross pairwise directional connectedness* from *j* to *i* is defined as follows:

$C_{i \leftarrow j}^H = d_{ij}^H.$

Since in general $C_{i\leftarrow j}^{H} \neq C_{j\leftarrow i}^{H}$, the *net pairwise directional connectedness* from *j* to *i*, can be defined as:

$$C_{ij}^{H} = C_{j\leftarrow i}^{H} - C_{i\leftarrow j}^{H}.$$

As for the off-diagonal row sums in Table 1, they give the share of the *H*-step forecast-error variance of variable x_i coming from shocks arising in other variables (all others, as opposed to a single other). The off-diagonal column sums provide the share of the *H*-step forecast-error variance of variable x_i going to shocks arising in other variables. Hence, the off-diagonal row and column sums, labelled "from" and "to" in the connectedness table, offer the total directional connectedness measures. In particular, *total directional connectedness from others to i* is defined as

$$C_{i\leftarrow\bullet}^{H} = \sum_{\substack{j=1 \\ j\neq i}}^{N} d_{ij}^{H},$$

and *total directional connectedness from j to others* is defined as

$$C_{\bullet\leftarrow j}^{H} = \sum_{\substack{i=1 \\ j\neq i}}^{N} d_{ij}^{H}.$$

We can also define *net total directional connectedness* as

$$C_{i}^{H} = C_{\bullet\leftarrow i}^{H} - C_{i\leftarrow\bullet}^{H}.$$

Finally, the grand total of the off-diagonal entries in D^H (equivalently, the sum of the "from" column or "to" row) measures *total connectedness*:

$$C^{H} = \frac{1}{N}\sum_{\substack{i,j=1 \\ j\neq i}}^{N} d_{ij}^{H}.$$

For the case of non-orthogonal shocks, the variance decompositions are not as easily calculated as before, because the variance of a weighted sum is not an appropriate sum of variances. Otherwise, methodologies for providing orthogonal innovations like traditional Cholesky-factor identification may be sensitive to ordering. Therefore, following Diebold and Yilmaz (2014), a generalized VAR decomposition (GVD), which is invariant to ordering, proposed by Koop *et al.* (1996) and Pesaran and Shin (1998) will be used. The *H*-step generalized variance decomposition matrix is defined as $D^{gH} = \left[d_{ij}^{gH} \right]$, where

$$d_{ij}^{gH} = \frac{\sigma_{jj}^{-1} \sum_{h=0}^{H-1} \left(e_i' \Theta_h \Sigma e_j \right)^2}{\sum_{h=0}^{H-1} \left(e_i' \Theta_h \Sigma \Theta_h' e_i \right)} \tag{2}$$

In this case, e_j is a vector with *j*th element unity and zeros elsewhere; Θ_h is the coefficient matrix in the infinite moving-average representation from VAR; Σ is the covariance matrix of the shock vector in the non-orthogonalized-VAR, σ_{jj} being its *j*th diagonal element. In this GVD framework, the lack of orthogonality means that the rows of d_{ij}^{gH} do not have sum unity and, in order to obtain a generalized connectedness index $\tilde{D}^g = \left[\tilde{d}_{ij}^g \right]$, the following normalization is necessary: $\tilde{d}_{ij}^g = \frac{d_{ij}^g}{\sum_{j=1}^{N} d_{ij}^g}$, where by construction $\sum_{j=1}^{N} \tilde{d}_{ij}^g = 1$ and $\sum_{i,j=1}^{N} \tilde{d}_{ij}^g = N$.

The matrix $\tilde{D}^g = \left[\tilde{d}_{ij}^g \right]$ permits us to define similar concepts as defined before for the orthogonal case, that is, *total directional connectedness*, *net total directional connectedness*, and *total connectedness.*

It is worthily to note that the Diebold and Yilmaz's (2014) connectedness framework is closely linked with both modern network theory (see Glover and Richards-Shubik, 2014) and modern measures of systemic risk (see Ang and Longstaff, 2013 or Acemoglu *et al*., 2015). This framework has been used by Diebold and Yilmaz (2015) for defining, measuring, and monitoring connectedness in financial and related macroeconomic environments (cross-firm, cross-asset, cross-market, cross-country, etc.). The degree of connectedness, on the other hand, measures the contribution of individual units to systemic network events, in a fashion very similar to the conditional value at risk (CoVaR) of this unit (see, e.g., Adrian and Brunnermeier, 2016).

2.2 Dynamic connectedness based on TVP-VAR

Antonakakis and Gabauer (2017) extend and refine the current connectedness literature by applying TVP-VAR, instead of the currently proposed rolling-window VAR. This improves the methodology provided by Diebold and Yilmaz (2014) substantially, because under their proposed methodology: (1) there is no need to arbitrarily set the rolling window-size, (2) it employs the entire sample to estimate the dynamic connectedness so there is no major loss of observations, and (3) it is not outlier sensitive. Another advantage of their proposed TVP-VAR-based measure of connectedness is that it adjusts immediately to events.

The TVP-VAR methodology allows both the VAR parameters and the variances to vary via a stochastic volatility Kalman Filter estimation with forgetting factors introduced by Koop and Korobilis (2014). As such, this approach can also be conducted to examine dynamic connectedness with limited time-series data.

The TVP-VAR model can be written as follows,

$$Y_t = \beta_t Y_{t-1} + \varepsilon_t, \quad \varepsilon_t \left| F_{t-1} \sim N\left(0, \sum_t\right)\right. \tag{3}$$

$$\beta_t = \beta_{t-1} + \nu_t, \quad \nu_t \left| F_{t-1} \sim N\left(0, R_t\right) \right. \tag{4}$$

Where β_t is an NxN_p dimensional time-varying coefficient matrix and ε_t is an $Nx1$ dimensional error disturbance vector with an NxN time varying variance-covariance matrix, Σ_t. The parameters β_t follow a random walk and depend on their own lagged values β_{t-1} and on an NxN_p dimensional matrix with an N_pxN_p variance-covariance matrix, R_t.[3]

The time-varying coefficients β_t and Σ_t can be used in the DY connectedness measure where the dynamic *H*-step generalized variance decomposition matrix is now

$$d_{ij,t}^{gH} = \frac{\sigma_{jj,t}^{-1} \sum_{h=0}^{H-1} \left(e_i' \Theta_{h,t} \Sigma_t e_j\right)^2}{\sum_{h=0}^{H-1} \left(e_i' \Theta_{h,t} \Sigma_t \Theta_{h,t}' e_i\right)} \tag{5}$$

Which after normalization would be $\tilde{d}_{ij,t}^{g} = \frac{d_{ij,t}^{gH}}{\sum_{j=1}^{N} d_{ij,t}^{gH}}$. Similarly, the matrix $\tilde{D}_t^g = \left[\tilde{d}_{ij,t}^{g}\right]$ permits us to define the dynamic *total directional connectedness, net total directional connectedness*, and *total connectedness.*

3. Data and preliminary analysis

We download close daily data on four volatility indices representative of the investors' consensus view of expected stock market volatility in the Standard & Poor's 500 Index. We make use of the CBOE Short-Term Volatility Index (VIX9D) to gauge market-based expectations of 9-day volatility. The CBOE Volatility Index (VIX) is employed to

[3] Following Koop and Korobilis (2014), we use the same non-informative initial conditions in the Kalman filter, a decay factor of 0.96 and a forgetting factor of 0.99 (see online appendix in Koop and Korobilis, 2014, for the technical details). Without loss of generality, we normalize the series, Y_t, to get a faster convergence in the Kalman filter and smoother. This normalization does not have any effect on the connectedness matrix.

measure expectations of 30-day future volatility. We utilize the CBOE 3-Month Volatility Index (VIX3M) to measure of 3-month implied volatility. Finally, the CBOE Mid-Term Volatility Index (VIX6M) is used as indicator of the expected volatility over a 6-month time horizon. All four indexes are calculated by the CBOE by applying the VIX methodology.[4] The data are collected from the CBOE website. Given that the GVD requires normality, and that volatilities tend to be distributed asymmetrically (with a right skew), we approximate normality by taking natural logarithms (see, e.g. Diebold and Yilmaz, 2015). Hence, we work with the logarithm of the daily implied-volatilities. Our sample spans from January 3, 2011 until May 4, 2018 (i.e., a total of 1,914 observations).

The Panel A of Table 2 presents the descriptive statistics for these series. As can be seen, the average log implied volatility in our sample decreases with the time horizon, being the VIX6M the highest and the VIX9D the lowest. The logarithm of our market volatility indices presents a positive skewness (suggesting that the distribution has a long right tail) and kurtosis slightly greater than 3 (indicating that the distribution has longer tails relative to the normal). However, these figures are close to the theoretical skewness and kurtosis of a normal distribution. We report the pairwise correlations in the Panel B of Table 2. As expected, these correlations are high, being not lower than 0.86. Intuitively, these high correlations could shed light about the connections between the implied-volatilities at different maturities, which we develop further below as the main goal of this paper.

[Insert Table 2 here]

Finally, Figure 1 shows the daily evolution in the logarithm of the implied volatilities under study. We can easily identify three salient characteristics: (a) sudden spikes, in

[4] See http://www.cboe.com/micro/vix/vixwhite.pdf

which volatility jumps from (relatively) low levels to (relatively) high ones; (b) slow exponential declines, which bring down volatility to more reasonable levels following a spike; and c) the spikes in the implied-volatility seems to coincide for all the maturities which also suggests a connection between them.

Note that the highest values of implied volatility occur when investors anticipate that huge movements in the Standard & Poor's 500 Index in either direction are likely. In these graphs, we observe several well-known peaks in volatilities, which coincide with important events, such as:

i) the debt ceiling crisis of August 2011, when the US Congress and White House clashed over raising the government borrowing limit, prompting a spike in economic policy uncertainty and a downgrading of US credit rating from AAA to AA+;

ii) China's bursting equity bubble and the subsequent international stock market sell-off in August 2015;

iii) the global financial turmoil after the UK voted to leave the European Union in June 2016; and

iv) the correction observed in early February 2018 triggered by market perceptions of rising inflation and a corresponding adjustment in monetary policy expectations.

[Insert Figure 1 here]

4. Empirical results

In this section, we report the empirical results of the implied volatility connectedness. First, we show the static or full-sample GVD table. Second, we analyze the dynamic connectedness through TVP-VAR.

4.1 Static (full-sample, unconditional) analysis

In the Table 3, we report the full-sample connectedness table where the off-diagonal elements measure the connectedness between the implied-volatility indices. As mentioned in Section 2, the *ij*th entry of the upper-left 4x4 market submatrix gives the estimated *ij*th pair-wise directional connectedness contribution to the forecast error variance of market *i*'s implied volatility coming from innovations to market *j*. Hence, the off-diagonal column sums (labelled TO) and row sums (labelled FROM) gives the total directional connectedness to all others from *i* and from all others to *i*, respectively. The bottom-most row (labelled NET) gives the difference in total directional connectedness (TO minus FROM). Finally, the bottom-right element (in boldface) is total connectedness, which is calculated as the sum of the non-diagonal elements of the connectedness matrix, divided by number of assets.[5]

[Insert Table 3 here]

As can be seen, the diagonal elements (own connectedness) are the largest individual elements in the table, ranging from 27.36% (VIX3M) to 28.78% (VIX6M). Interestingly, the own connectedness is smaller than any total directional connectedness FROM and TO others, reflecting that these implied volatilities are somewhat dependent of each other. Namely, news shocks that affect to the implied volatility of a particular maturity extensively spread on the implied volatilities of the other maturities. Accordingly, the total connectedness of implied volatilities is 72.27%, indicating that only a 27.73% of the variation is due to idiosyncratic shocks. This result is in line with the value of 78.3% obtained by Diebold and Yilmaz (2014) for the total connectedness

[5] All results are based on a VAR model of order 2 and generalized variance decompositions of 10-day ahead volatility forecast errors. To check for the sensitivity of the results to the choice of the order of VAR, we also calculate the spillover index for orders 2 through 4, as well as for forecast horizons varying from 4 days to 10 days. The main results of our paper are not affected by these choices. Detailed results are available from the authors upon request.

between US financial institutions, but lower than the value of 97.2% found by Diebold and Yilmaz (2012) for international financial markets.

Regarding to the net (TO minus FROM) contribution, our results suggest that the VIX9D is the only net receiver of implied volatility (-10.02%), being VIX, VIX3M and VIX6M net volatility triggers (4.48%, 3.85%, and 1.68%, respectively), suggesting that the volatility shocks of long maturities are spread on the shortest maturity. Finally, the highest observed net pairwise connectedness is from VIX to VIX9D (3.81%), followed by that from VIX3M to VIX9D (3.32%).

4.2 Dynamic analysis

The previous section provides a snapshot of the "unconditional", or full-sample, aspects of the connectedness measure among the implied volatility indices. However, the dynamics of the connectedness measures remains covered. The appeal of connectedness methodology lies in its use as a measure of how quickly volatility shocks spread across holding periods as well as within the same maturity. As previously stated, we carry out an analysis of dynamic connectedness based on TVP-VAR.

In the Figure 2, we report the evolution of the total connectedness between the four implied volatility indices.[6] Figure 2 also highlights several cycles of connectedness where the total connectedness is higher or lower than the full sample average. As expected, the connectedness index shows a time-varying pattern over the sample period. The most significant spikes are observed (i) in the end of 2011, where significant tensions where observed in a context of uncertainty about global economic growth; (ii) in the first few months of 2013, coinciding with political agreements to temporarily avoid the so-called fiscal cliff and raise the federal debt ceiling; (iii) in the second half of 2014, possibly associated with the rising of geopolitical tensions due to the

[6] To eliminate the effect of the non-informative initial conditions in the Kalman filter, we have skipped the first 200 days of the sample and plot the results from October 12, 2011 to May 4, 2018. This number is somehow arbitrary but conservative.

Russia/Ukraine conflict and concerns about the global growth outlook; (iv) in the middle of 2015, reflecting uncertainty surrounding events in Greece and the sharp declines in Chinese equity prices, which (coupled with a rapid fall in oil prices) raised concerns about the global economic outlook; and in February 2018, in a context of significant correction of share prices which caused the decease of volatility ETFs such as XIV[7], following the sudden signs of an increase in wage inflation in the United States. Interestingly, there are also important reductions in connectedness during our sample in February 2012 (corresponding to Greek government-debt crisis), in September 2012 (after a series of terrorist attacks are directed against United States diplomatic missions worldwide, as well as diplomatic missions of Germany, Switzerland and the United Kingdom), in June 2016 (when the United Kingdom voted in a referendum to leave the European Union), in January 2017 (after Donald Trump sword in as the 45th President of the United States), and in August 2017 (in an environment of favourable economic activity figures, contained inflation and abundant liquidity built up after several years of highly expansionary monetary policies).

As can be seen, triggers of connectedness intensity among the implied volatility indices under study can come in many different shapes and sizes (policy uncertainty, geopolitical unrest, etc.), since the effects of these triggers on particular investors depend on their time horizon. Indeed, some events can increase the perceived volatility in a given investment horizon, but not in the others, depending on how much risk an investor is exposed and her expectations about the future evolution after the event. For example, the appointment of Donald Trump as president of the US affected investors with a short time horizon (VIX9D and VIX), but investors with longer time horizons

[7] https://www.cnbc.com/2018/02/06/the-obscure-volatility-security-thats-become-the-focus-of-this-sell-off-is-halted-after-an-80-percent-plunge.html

were not so influenced because they would have thought that the potential disruptive change would dissipate with the passage of time.

Therefore, the "unconditional", or full-sample, total connectedness of 72.27% that we report in the previous section actually undervalues the potential connectedness of the implied volatilities indices. These indices seem to be more connected in periods of high market stress with potential effect across the whole range of investors' time horizons, making them most vulnerable to contagion.

5. Net directional connectedness

5.1. Net directional volatility connectedness plots

The net directional connectedness index provides information about how much each market's volatility with certain maturity contributes in net terms to other maturities. As the dynamic total connectedness measure presented in Section 4.2, it also relies on the TVP-VAR connectedness approach. Figure 3 displays the dynamic net connectedness.

[Insert Figure 3]

As can be seen, our results suggest that VIX9D (blue line) was net absorber of volatility throughout the sample, and VIX (black line), VIX3M (red line) and VIX6M (green line) were net volatility propagators during the most of the sample (being -12.78% and 4.08%, 4.94%, 3.75%, respectively, their estimated average net directional connectedness in Figure 3). Remarkably, the net directional volatility connectedness for VIX9D fluctuated substantially within a band of (-1.20%, -56.16%), reaching the minimum level, -56.16%, coinciding with the reintensification of the euro area sovereign debt crisis in the late spring of 2012[8]. Regarding, VIX, VIX3M and VIX6M are net receivers of volatility during short periods of the sample, being their minimum

[8] Recall that VIX9D provides a market-based gauge of expectations of 9-day volatility, making it particularly responsive to the short term changes in the S&P 500 Index.

net directional volatility connectedness of -3.23% (August 2013), -2.10% (May 2015) and -4.96% (December 2015), respectively.

A further inspection of Figure 3 indicates the existence of at least three significant subperiods of intense transmission of volatility: (a) from December 2011 to July 2012, when concerns about the political and financial stability of the euro area re-emerged and triggered renewed flight-to-safety flows and widening spreads for some euro area government bonds[9]; (b) from May to July 2014, reflecting rising geopolitical tensions and concerns about the global growth outlook; and (c) from November 2016 to May 2017, when the equity risk premium remained significantly higher than before the onset of the financial crisis in 2008.

5.2. Dynamic net pair-wise directional volatility connectedness plots

So far, we have discussed the behavior of the total connectedness and total net directional connectedness measures for the four implied volatility indices with different maturities. However, we have also examined their net pairwise directional connectedness during the financial turmoil periods experienced in the sample period. By construction, the net directional connectedness from implied volatility *i*-th to others is equal to the sum of all the net pair-wise connectedness from implied volatility *i*-th to implied volatility *j*-th, for all *j* with $i \neq j$, i.e. $C_i^H = \sum_{\substack{j=1 \\ j \neq i}}^{N} \left(\tilde{d}_{ji}^H - \tilde{d}_{ij}^H \right)$. Having this relationship in mind, in Figures 4 to 7, the dynamics of the net pairwise directional connectedness of the implied volatility with maturity *i*-th with respect to the other maturities under study are added to the net directional connectedness (grey area) explained before. This decomposition of the dynamics of net directional connectedness into their pairwise directional connectedness is appealing since it allows a deeper

[9] These concerns were mainly fueled by the outcome of the Greek elections in May, by a number of downgrades of Spanish and Italian banks and by Moody's downgrade of the Spanish sovereign rating in June.

understanding how the transmission of volatility works for each implied volatility index.

As can be seen in Figure 4, VIX9D was completely a net absorber of volatility from all the implied volatility indices, being all the computed values negatives in our sample. As can be seen (Figures 5-7, blue line), the net pair-wise directional volatilities to VIX9D from VIX, VIX3M and VIX6M highlight how there may exist direct mechanisms of volatility transmission to the short-term volatility index from higher time horizons in at least three significant subperiods of intense transmission of volatility as commented before. One can note its net pair-wise directional volatilities were declining gradually around this period until reaching the lowest values, -23.01%, -16.81% and -16.36% in late March 2012, respectively (corresponding to Greek government-debt crisis). Moreover, in the second half of 2014 (associated with the rising of geopolitical tensions due to the Russia/Ukraine conflict and concerns about the global growth outlook), and in January 2017 (after Donald Trump was inaugurated as the President of the United States) the behaviour is analogous.

[Insert Figure 4]

In Figure 5, we observe that VIX was mostly a net trigger of volatility to VIX9D over all time periods. Interestingly, the short episodes where VIX shows swing in net volatility where periods of net generator of volatility are followed by periods where this is net receiver of volatility, e.g., in the period May 2013-January 2014. This period coincides with an episode of heightened uncertainty and renewed volatility in global financial markets following suggestion by the Chairman of the US Federal Open Market Committee of the likelihood that the Federal Reserve System would be tapering its asset purchase programme. The transmission of volatility to VIX from VIX3M and VIX6M persisted until the beginning of 2015, highlighting that, despite improving real

economic outlooks, market participants considered that vulnerabilities still remained. Likewise, VIX was net receiver of volatility from higher time horizons during much of the sample, except from the first months of 2015 to late 2016, reflecting the episodes of heightened uncertainty and short-lived peaks in financial market volatility following the UK referendum on EU membership in June and the US presidential election in November. Immediately after that, the net pair-wise directional connectedness from VIX3M and VIX6M to VIX were decreasing slowly until reaching low values, -3.67% and -3.50%, respectively, being this behaviour possibly related with political uncertainty after the U.S. presidential election. Finally, VIX turned into net transmitter of volatility to VIX6M remained a net receiver of volatility from VIX3M from March 2017 until the end of the sample, in a context of low financial market volatility, elevated asset valuations and compressed risk premia, pointing to increased risk-taking.

[Insert Figure 5]

Regarding VIX3M (Figure 6), as can be seen, it was net generator of volatility to all other implied volatility indices most of the sample. It is interesting to note that the two episodes when VIX3M is net receiver of volatility (April-June 2015 and January-March 2016), the main trigger of volatility to VIX3M is VIX, although during the first of two VIX6M had a negative influence.

[Insert Figure 6]

Finally, Figure 7 reports the results for VIX6M. VIX6M was a strong trigger of volatility to VIX9D over all time periods, but also to VIX from the beginning until 2015 as described above. Furthermore, the VIX6M was a net receiver of volatility from VIX3M whose net pairwise volatility to VIX was decreasing gradually along 2013, reverting this trend at the end of that year after the Federal Reserve indicated its willingness to start scaling back its bond purchases. Interestingly, the two episodes

where VIX6M was net receiver of volatility (October 2015-January 2016 and January 2018-May 2018), both of them are linked to the net pair-wise volatilities from VIX and VIX3M: while the first period could be associated with increased fears of a renewed global slowdown, the second period could be related with a significant correction of share prices, following the sudden signs of an increase in wage inflation in the United States in February 2018.

[Insert Figure 7]

In summary, Figures 4 to 7 have shown how the dynamics of the net pair-wise connectedness between all the volatility indices are not constant but switching from net generator to net receiver of volatility to other, depending on either time horizons. Therefore, the unconditional or full-sample connectedness measure is not able to uncover all the dynamics of the connectedness between the implied volatility indices at different maturities.

6. Robustness checks

To provide robustness to the previous results, in this Section, we successively make use of the generalized impulse-response functions (GIRF) to further evaluate the relationship between the implied volatility indices under study. In addition, we compare the dynamic total connectedness obtaining using both Diebold and Yilmaz (2014)'s original connectedness approach via rolling windows and the alternative TVP-VAR connectedness approach developed by Antonakakis and Gabauer (2017).

6.1 Generalized impulse-response functions.

Since the Cholesky-factor identification may be sensitive to ordering, once again, we make use of a generalized VAR decomposition, invariant to ordering, proposed by Koop *et al.* (1996) and Pesaran and Shin (1998) of our VAR system in Equation (1).

GIFR traces out the responsiveness of the dependent variable in the VAR to shocks to each of the variables.

To easy interpretation, the graphs in Figure 8 show the standardized impact of one standard deviation shock to the individual implied volatility of certain maturity on its own and those of the other maturities on one year, or a 250-day forecasting horizon. These results should be interpreted with care as they have been produced in the generalized VAR framework that impairs the orthogonality of shocks affecting the individual implied volatility indices at different holding periods (Antonakakis and Vergos, 2013). In any case, these generalized impulse-response functions are simply indicative of the impact of future shocks.

[Insert Figure 8]

In short, we observe how shocks to any maturity have a strong effect on itself and on the other maturities of similar magnitude. However, this effect dies off quicker, the shorter the maturity of the implied volatility.

6.2 Dynamic connectedness: TVP-VAR versus 200-day rolling windows

Finally, we compare the dynamic total connectedness based on TVP-VAR with that of the standard approach in the connectedness literature, which consists in applying the Diebold-Yilmaz connectedness methodology based on overlapping 200-day rolling windows. Figure 9 plots the dynamic total connectedness with both approaches.

[Insert Figure 9]

As it can be seen, although both approaches track each other well (with a significant Pearson correlation of 24%), the TVP-VAR is able to pick up changes in the connectedness earlier than the rolling windows approach. Hence, we confirm the superiority of the TVP-VAR at tracking changes in the connectedness. This feature is related to the fact that the latter could be capturing the changing market participants'

expectations, being therefore able to identify substantially different episodes of connectedness intensification, yielding more accurate and sensible indicators of the spread of market disturbances between different time investment horizons.

7. Concluding remarks

With a strong understanding of volatility and its causes, investors potentially can take advantage of investment opportunities resulting from volatile markets. Over the last two decades, the demand for volatility derivative products has grown exponentially, driven in part by the need to hedge volatility risk in portfolio management. Since risk may be significantly different for different investment horizons, the transmission of volatility at different maturities has important implications for asset allocation decisions.

In this paper, we have investigated interconnection between four implied volatility indices representative of the investors' consensus view of expected stock market volatility at different holding horizons during the period January 3, 2011-May 4, 2018. To that end, we make use of both the original connectedness approach proposed by Diebold and Yilmaz (2014) and the TVP-VAR connectedness approach developed by Antonakakis and Gabauer (2017). In particular, we have focused the interdependence between CBOE implied volatility indices representative of 9-day, 30-day, 3-month and 6-month time horizons.

By making especial emphasis in the dynamic analysis of implied volatility transmission between investment time horizons during the successive of financial crises registered during the sample period, our study may enhance the understanding of time fear connectedness dynamics in times of both turbulence and calm, and may help to assess the perceived risk of crisis transmission.

The main findings of our research can be summarized as follows. In the first step, we found a system-wide value of 72.27% for the total connectedness between the four implied volatility indices under study for the full sample period. This level is in line with that obtained by Diebold and Yilmaz (2014) for US financial institutions. In the second step, we analysed the dynamic nature of total net connectedness, obtaining evidence of spillovers, showing large variation over time and supporting the literature documenting that volatility across markets increases during times of financial turbulence, making the real-time detection of instability an important practical issue (see, e. g., Shi *et al*., 2018). In a third step, we examined the time-varying net spillovers across markets, observing in all cases that the implied volatility indices frequently switch between a net transmitting and a net receiving role. Furthermore, when using generalized impulse-response functions to alternatively evaluate the relationship between the implied volatility indices under study, we observe how shocks to any maturity have a strong effect on itself and on the other maturities of similar magnitude. Finally, we compare the time-varying connectedness using the traditional and the TVP-VAR approaches, confirming the superiority of the latter.

Our results may be of interest to policy-makers or portfolio risk managers, who should take into consideration the spillover effects detected by the dynamic interdependences between the implied volatility indices under study. Indeed, the connectedness measure can be used in a static or dynamic context, by showing the state of potential contagion among different time horizons at a certain point in time.

A natural extension to the analysis presented in this paper would be to explore the main determinants of the detected net directional connectedness, with special emphasis in the economic and institutional factors. This is an item in our future research agenda.

Acknowledgements

We thank Gary Koop and Dimitris Korobilis for providing the TVP-VAR programs.

Funding

This paper is based on work supported by the Spanish Ministry of Economy and Competitiveness [grant ECO2016-76203-C2-2-P].

References

Acemoglu, D., Ozdaglar, A. and Tahbaz-Salehi, A. (2015). Systemic risk and stability in financial networks. American Economic Review 105, 564-608.

Adrian, T. and Brunnermeier, M. (2016). CoVaR. American Economic Review 106, 1705-1741.

Ang, A. and Longstaff, F. A. (2013). Systemic sovereign credit risk: Lessons from the US and Europe. Journal of Monetary Economics 60, 493-510.

Antonakakis, N. and Gabauer, D. (2017). *Refined Measures of Dynamic Connectedness based on TVP-VAR.* MPRA, Working Paper No. 78282.

Antonakakis, N. and Vergos, K. (2013). Sovereign bond yield spillovers in the Euro zone during the financial and debt crisis. Journal of International Financial Markets, Institutions and Money 26, 258-272.

Baker, S. R., Bloom, N. and Davis, S. J. (2016). Measuring economic policy uncertainty. Quarterly Journal of Economics 131:, 593–636.

Banerjee, P. S., Doran, J. S. and Peterson, D. R. (2007). Implied volatility and future portfolio returns. Journal of Banking and Finance 31, 3183-3199.

Blair, B. J., Poon, S. and Taylor, S. J. (2001). Forecasting S&P 100 volatility: The incremental information content of implied volatilities and high-frequency index returns. Journal of Econometrics 105, 5-26.

Bloom, N., Floetotto, M., Jaimovich, N., Saporata-Eksten, T. and Terry, S. (2018). Really Uncertain Business Cycles. Econometrica 86, 1031-1065.

Branger, N., Hülsbusch, H. and Kraftschik, A. (2017). The Volatility-of-Volatility Term Structure. Presented at the joint the 70th European Meeting of the Econometric Society and the 32nd Annual Congress of the European Economic Association, Lisbon.

Campbell, John Y. (2000). Asset pricing at the millennium. Journal of Finance 55, 1515-1567.

Campbell, J. Y. and Viceira, L. (2005). The term structure of the risk-return tradeoff. Financial Analysts Journal 61, 34-44.

Carr, P. and Madan, D. (1998). Towards a theory of volatility trading, in R. A. Jarrow (Ed.) Risk Book on Volatility, New York: Risk, pp. 417-427.

Carr, P. and Lee, R. (2009). Volatility Derivatives. Annual Review of Financial Economics 1, 319-339.

Christenssen, B., and Prabhala, N. (1998). The relation between implied and realized volatility. Journal of Financial Economics 50, 125-150.

Christoffersen, P. F. and Diebold, F. X. (2000). How Relevant is Volatility Forecasting for Financial Risk Management? Review of Economics and Statistics 82, 12-22

Demeterfi, K., Derman, E., Kamal, M. and Zou, J. (1999). A guide to volatility swaps. Journal of Derivatives 7, 9-32.

Diebold, F. X. and Yilmaz, K. (2012). Better to give than to receive: Predictive directional measurement of volatility spillovers. International Journal of Forecasting 28, 57-66.

Diebold, F. X. and Yilmaz, K. (2014). On the network topology of variance decompositions: Measuring the connectedness of financial firms. Journal of Econometrics 182, 119–134.

Diebold, F. X. and Yilmaz, K. (2015). Financial and Macroeconomic Connectedness: A Network Approach to Measurement and Monitoring. Oxford: Oxford University Press.

Engle, R., Ghysels, E. and Sohn, B. (2013). Stock market volatility and macroeconomic fundamentals. Review of Economics and Statistics 95, 776–797.

Fleming, J. (1998). The quality of market volatility forecasts implied by S&P 100 index option prices. Journal of Empirical Finance 5, 317–345.

Giot, P. (2005). Relationships between implied volatility indexes and stock index returns. Journal of Portfolio Management 26, 12–17.

Glover, B. and Richards-Shubik, S. (2014). Contagion in the European Sovereign Debt Crisis. Working Paper20567. National Bureau of Economic Research, Cambridge, MA.

Gonzalez-Perez, M.T. (2015). Model-free volatility indexes in the financial literature: a review. International Review of Economics and Finance 40, 141-159.

Guo, H. and Whitelaw, R. F. (2006). Uncovering the risk-return relation in the stock market. Journal of Finance 61, 1433-1463.

Jabłecki,J., Kokoszczyński, R., Sakowski, P., Ślepaczuk, R. and Wójcik, P. (2014). Does historical VIX term structure contain valuable information for predicting VIX futures? Dynamic Econometric Models 14, 5-28

Jiang, G. J. and Tian, Y. S. (2005). Model-free implied volatility and its information con-tent. Review of Financial Studies 18, 1305-1342.

Johnson, T. L. (2017). Risk premia and the VIX term structure. Journal of Financial and Quantitative Analysis 52, 2461-2490

Jorion, P. (1995). Predicting volatility in the foreign exchange market. Journal of Finance 50, 507-528.

Koop, G. and Korobilis, D. (2014). A new index of financial conditions. European Economic Review 71, 101-116.

Koop, G., Pesaran, M. H. and Potter, S. M. (1996). Impulse response analysis in non-linear multivariate models. Journal of Econometrics 74, 119–147.

Lu, Z. and Zhu, Y. (2010). Volatility components: the term structure dynamics of VIX futures. The Journal of Futures Markets 30, 230–256.

Mankiw, G. and Reis, R. (2002). Sticky Information versus Sticky Prices: A Proposal to Replace the New Keynesian Phillips Curve, Quarterly Journal of Economics, 117, 1295-1328.

Morris, S. and Shin, H. (2002). Social value of public information. American Economic Review 92, 1521-1534.

Pesaran, M. H. and Shin, Y. (1998). Generalized impulse response analysis in linear multivariate models. Economics Letters 58, 17–29.

Poon, S. and Granger, C. W. J. (2003). Forecasting financial market volatility: A review. Journal of Economic Literature 41, 478-539.

Shi, S., Phillips P. C. B. and Hurn, S. (2018). Change detection and the causal impact of the yield curve. Journal of Time Series Analysis Special Issue, 1-22.

Whaley, R. E. (2000). The investor fear gauge. Journal of Portfolio Management 26,12–17.

Whaley, R. E., (2009). Understanding the VIX. Journal of Portfolio Management 35, 98–105.

Xu, X. and Taylor, S. J. (1995). Conditional volatility and the informational efficiency of the PHLX currency options markets. Journal of Banking and Finance 19, 803-821.

Table 1: Schematic connectedness table

	x_1	x_2	…	x_N	**Connectedness from others**
x_1	d_{11}^H	d_{12}^H	⋯	d_{1N}^H	$\sum_{j=1}^{N} d_{1j}^H, j \neq 1$
x_2	d_{21}^H	d_{22}^H	⋯	d_{2N}^H	$\sum_{j=1}^{N} d_{2j}^H, j \neq 2$
.	.	.	.		
.	.	.	.		
.	.	.	.		
x_N	d_{N1}^H	d_{N2}^H	⋯	d_{NN}^H	$\sum_{j=1}^{N} d_{Nj}^H, j \neq N$
Connectedness to others	$\sum_{i=1}^{N} d_{i1}^H$ $i \neq 1$	$\sum_{i=1}^{N} d_{i2}^H$ $i \neq 2$	⋯	$\sum_{i=1}^{N} d_{iN}^H$ $i \neq N$	**Total connectedness =** $\frac{1}{N}\sum_{i,j=1}^{N} d_{iN}^H$ $i \neq j$

Table 2: Descriptive statistics and contemporaneous correlations of implied volatilities

	VIX9D	VIX	VIX3M	VIX6M
Panel A: Descriptive statistics				
Mean	2.6960	2.7466	2.8696	2.9623
Std. Dev.	0.3498	0.2902	0.2360	0.2041
Min	1.9601	2.2127	2.4723	2.6210
Median	2.6599	2.7057	2.8291	2.9242
Max	4.2195	3.8712	3.7700	3.7223
Skewness	0.7522	0.9395	0.9947	0.9815
Kurtosis	3.7403	4.0836	4.1119	3.9515
Observations	1,914	1,914	1,914	1,914

Panel B: Matrix correlations							
	VIX9D		**VIX**		**VIX3M**		**VIX6M**
VIX9D	1						
VIX	0.9729	***	1				
VIX3M	0.9154	***	0.9736	***	1		
VIX6M	0.8577	***	0.9302	***	0.9856	***	1

Notes:

All the series are in logs.
Daily data from January 3, 2011 to May 4, 2018.
*** indicates significance at the 1% level

Table 3: Full-sample connectedness

	VIX9D	**VIX**	**VIX3M**	**VIX6M**	**Directional *FROM* Others**
VIX9D	27.39	26.71	23.77	22.13	72.61
VIX	22.90	27.39	25.50	24.21	72.61
VIX3M	20.45	25.63	27.36	26.56	72.64
VIX6M	19.25	24.75	27.23	28.78	71.22
Directional *TO* Others	62.60	77.09	76.49	72.91	**Total connectedness** =72.27
Net Contribution (To – From) Others	-10.01	4.48	3.85	1.68	

Figure 1: Daily financial market volatilities (in logs)

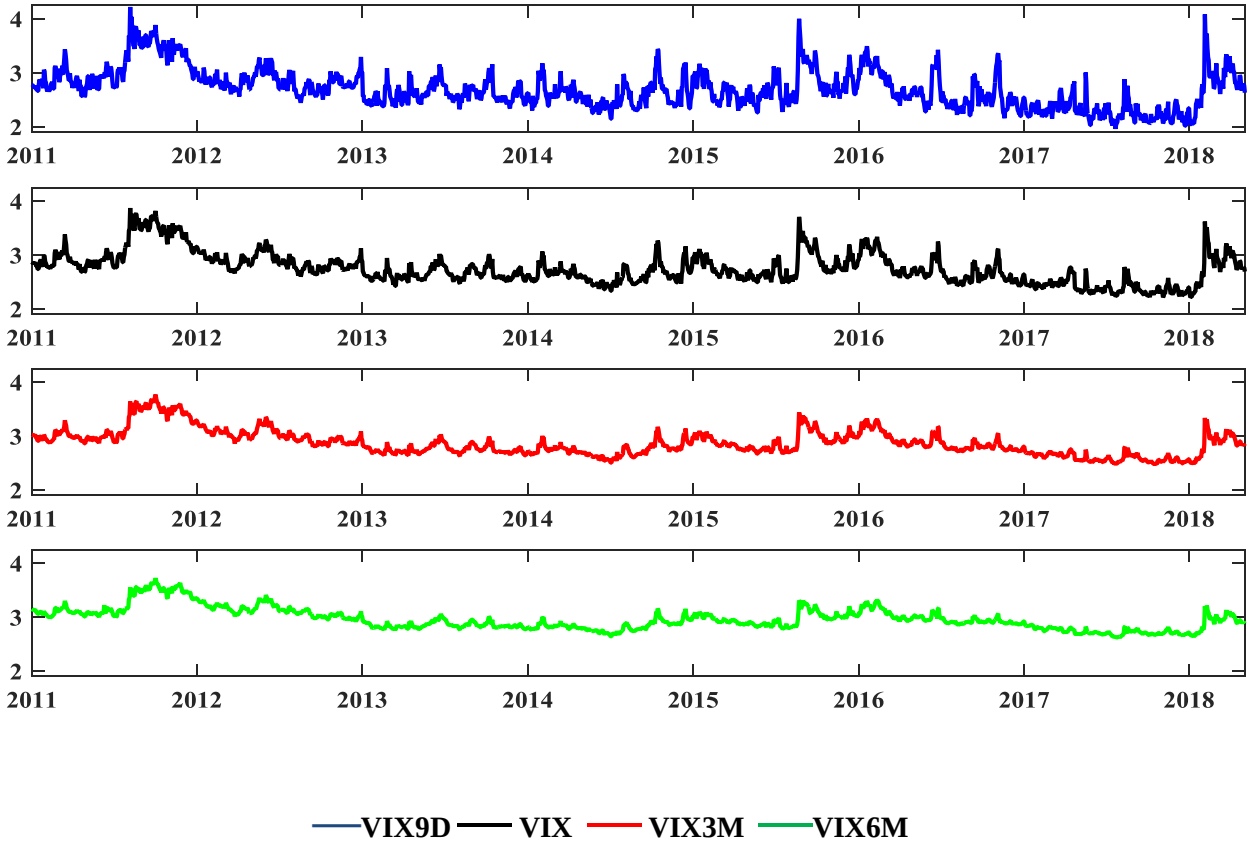

Figure 2: Dynamic total connectedness

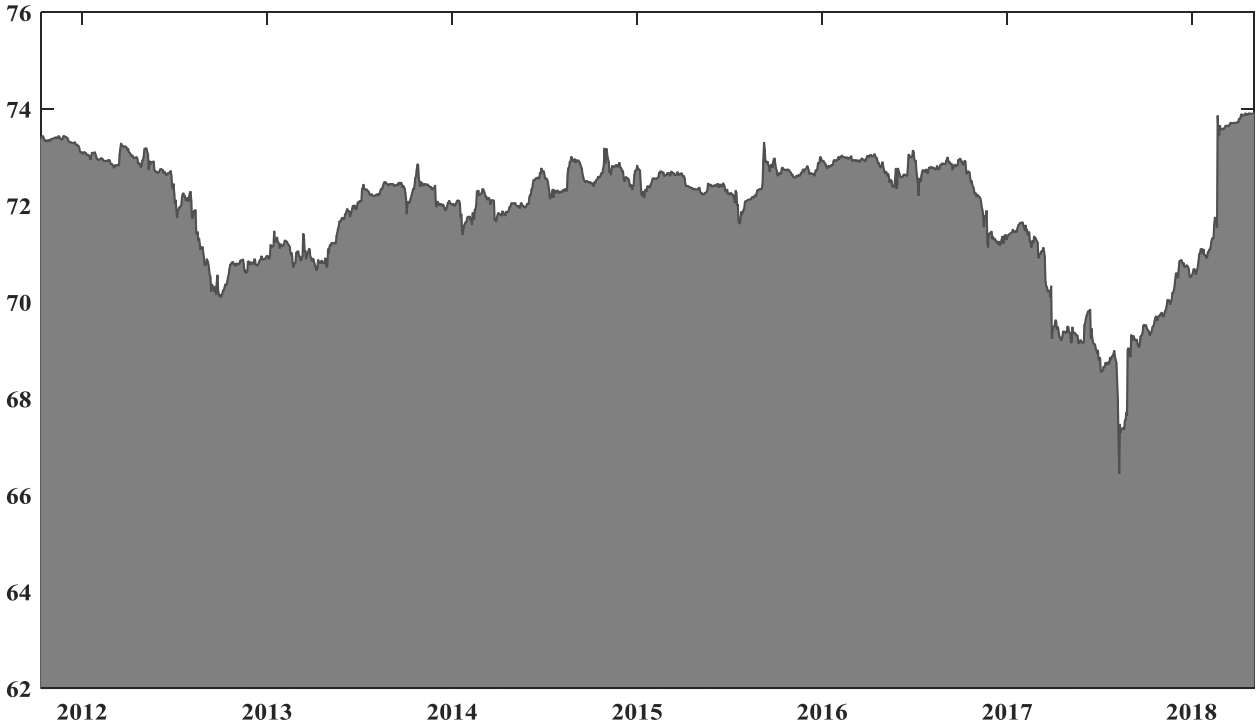

Note: The rolling estimation window width is 200 days, and the predictive horizon for the underlying variance decomposition is 10 days.

Figure 3: Net directional connectedness

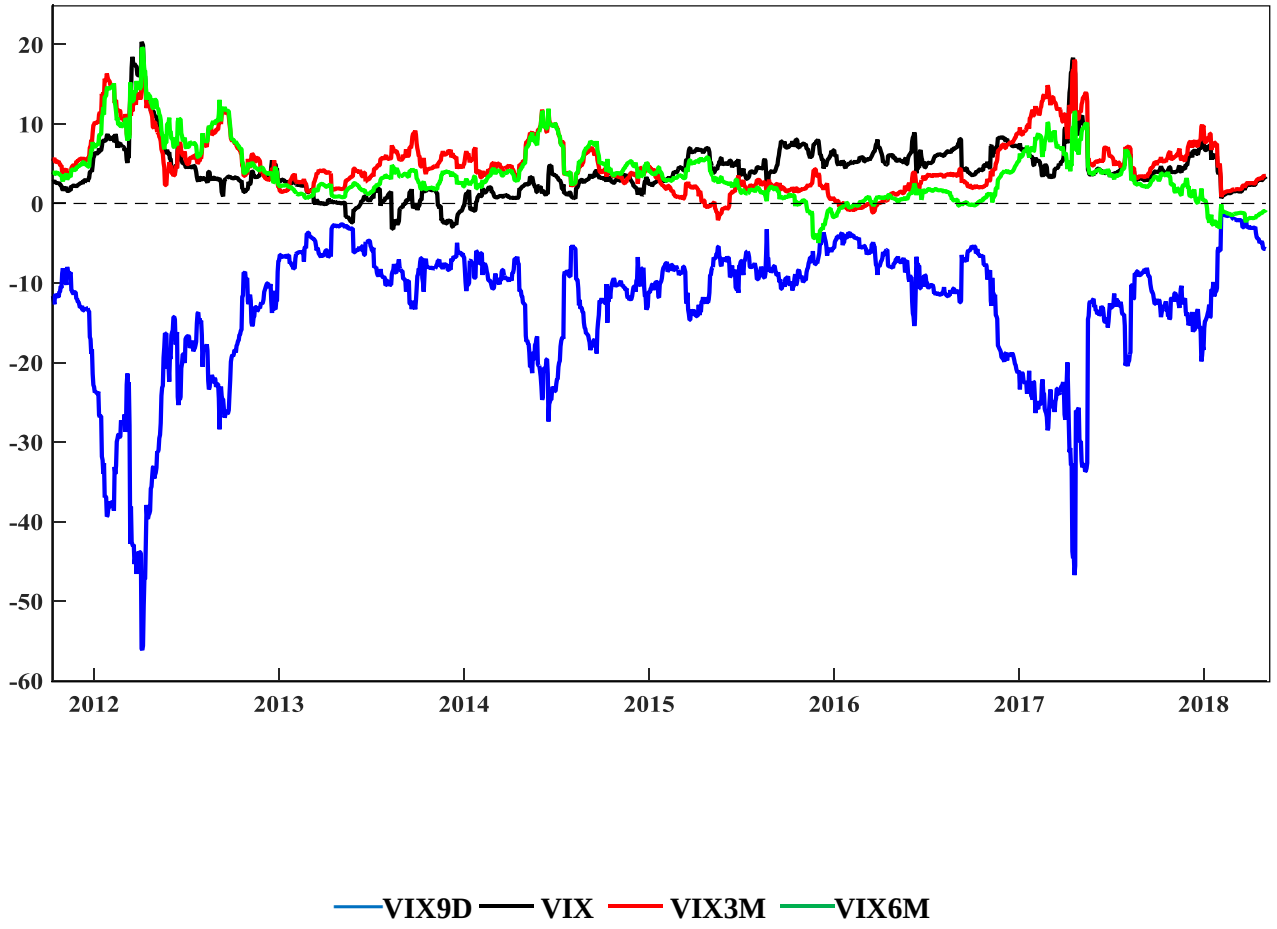
20
10
0
-10
-20
-30
-40
-50
-60
2012
2013
2014
2015
2016
2017
2018
VIX9D
VIX
VIX3M
VIX6M

Figure 4: Net directional connectedness and net pair-wise directional connectedness:

CBOE Short-Term Volatility Index (VIX9D Index)

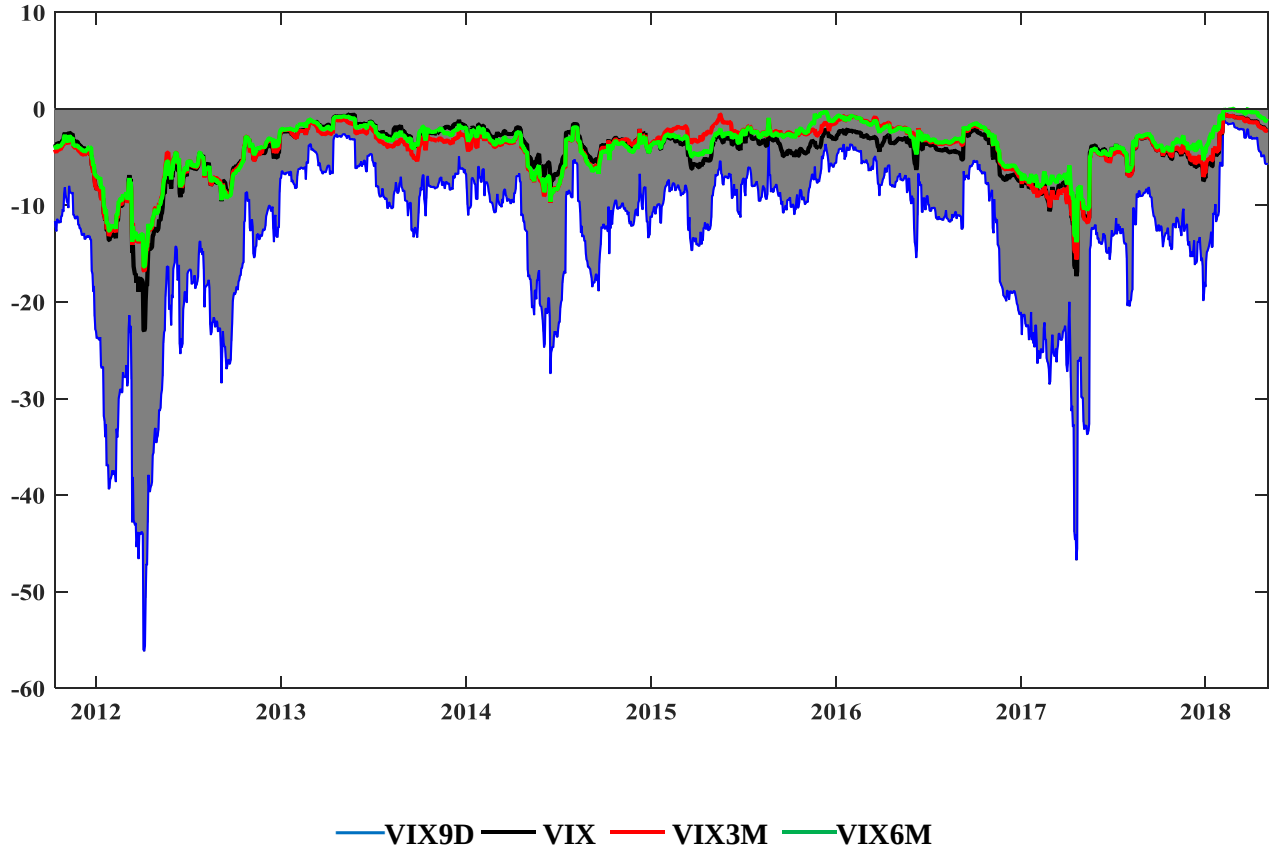

:

Figure 5: Net directional connectedness and net pair-wise directional connectedness: CBOE Volatility Index (VIX Index)

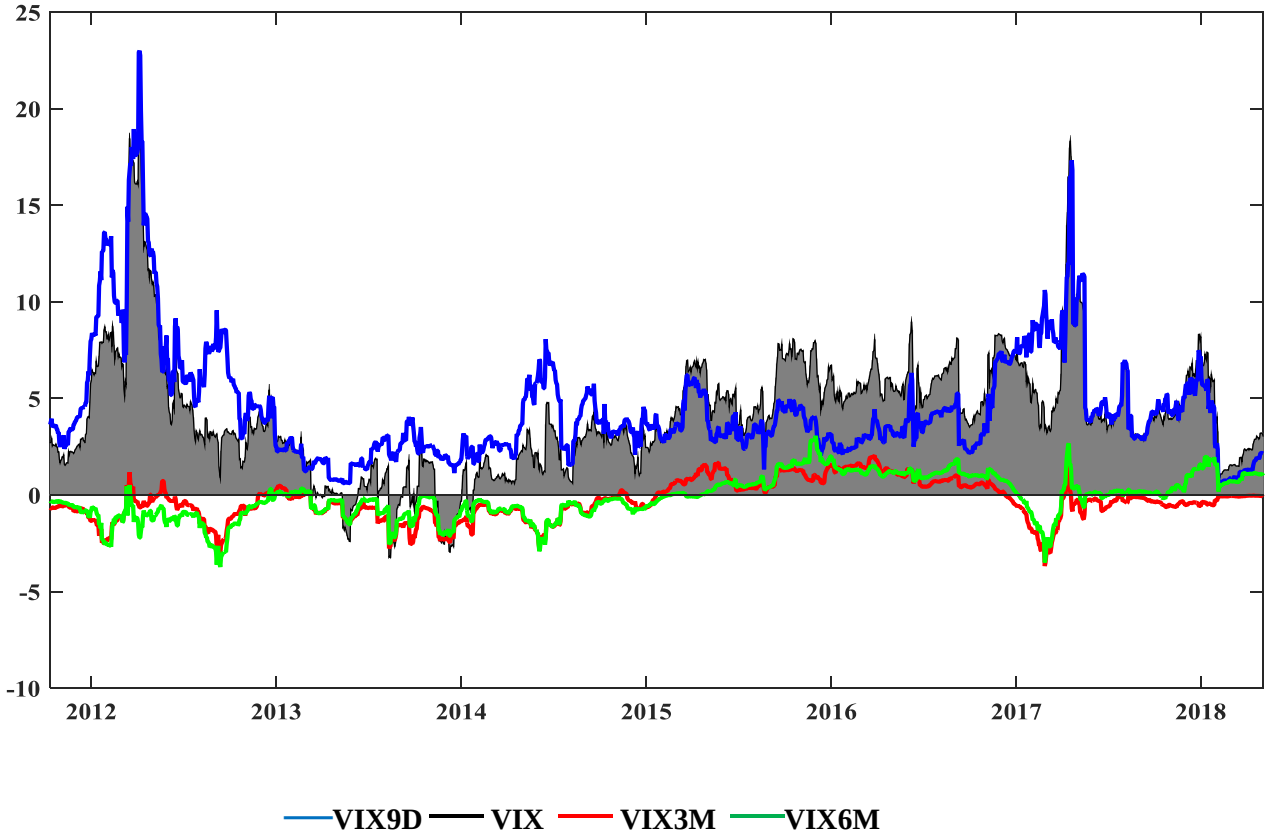

Figure 6: Net directional connectedness and net pair-wise directional connectedness:

CBOE 3-Month Volatility Index (VIX3M Index)

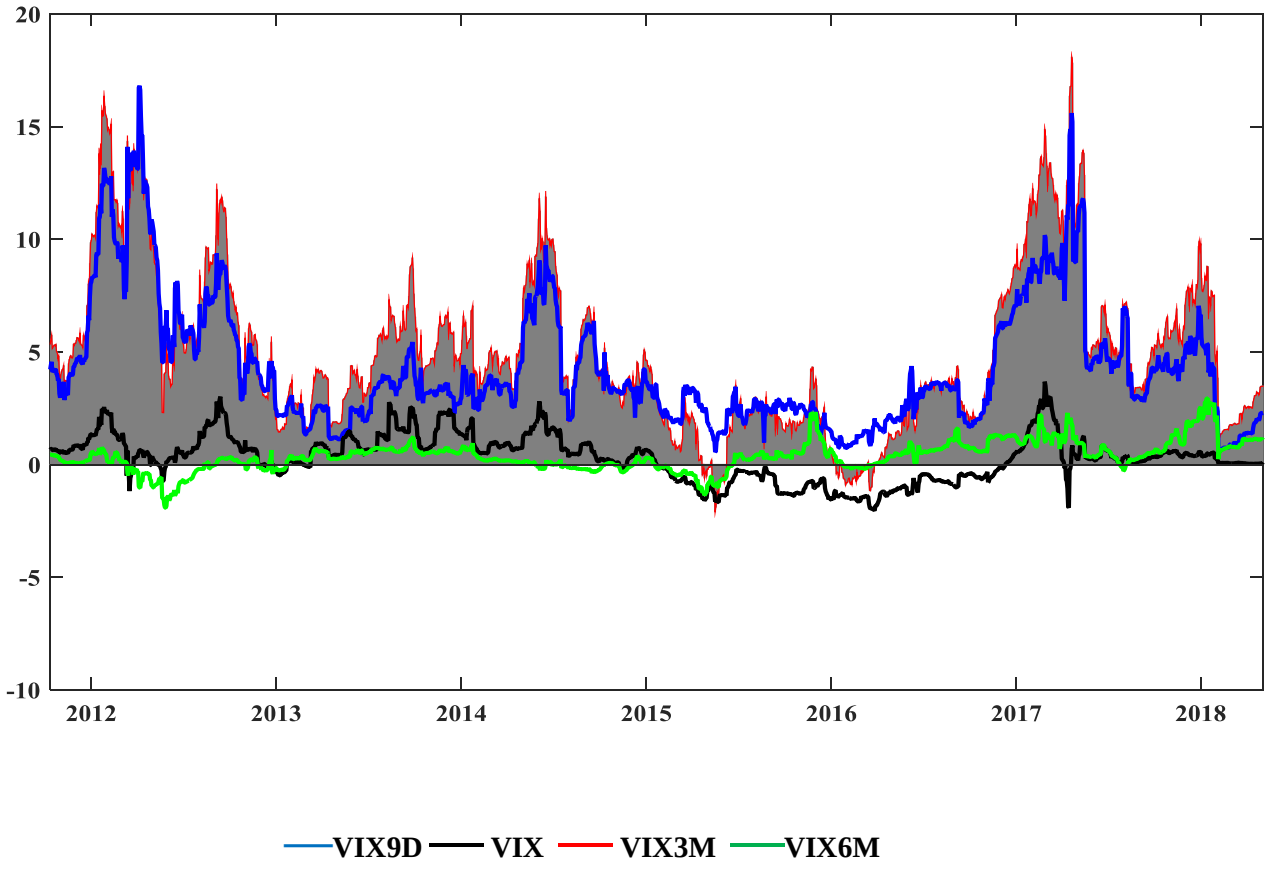

Figure 7: Net directional connectedness and net pair-wise directional connectedness:

CBOE Mid-Term Volatility Index (VIX6M Index)

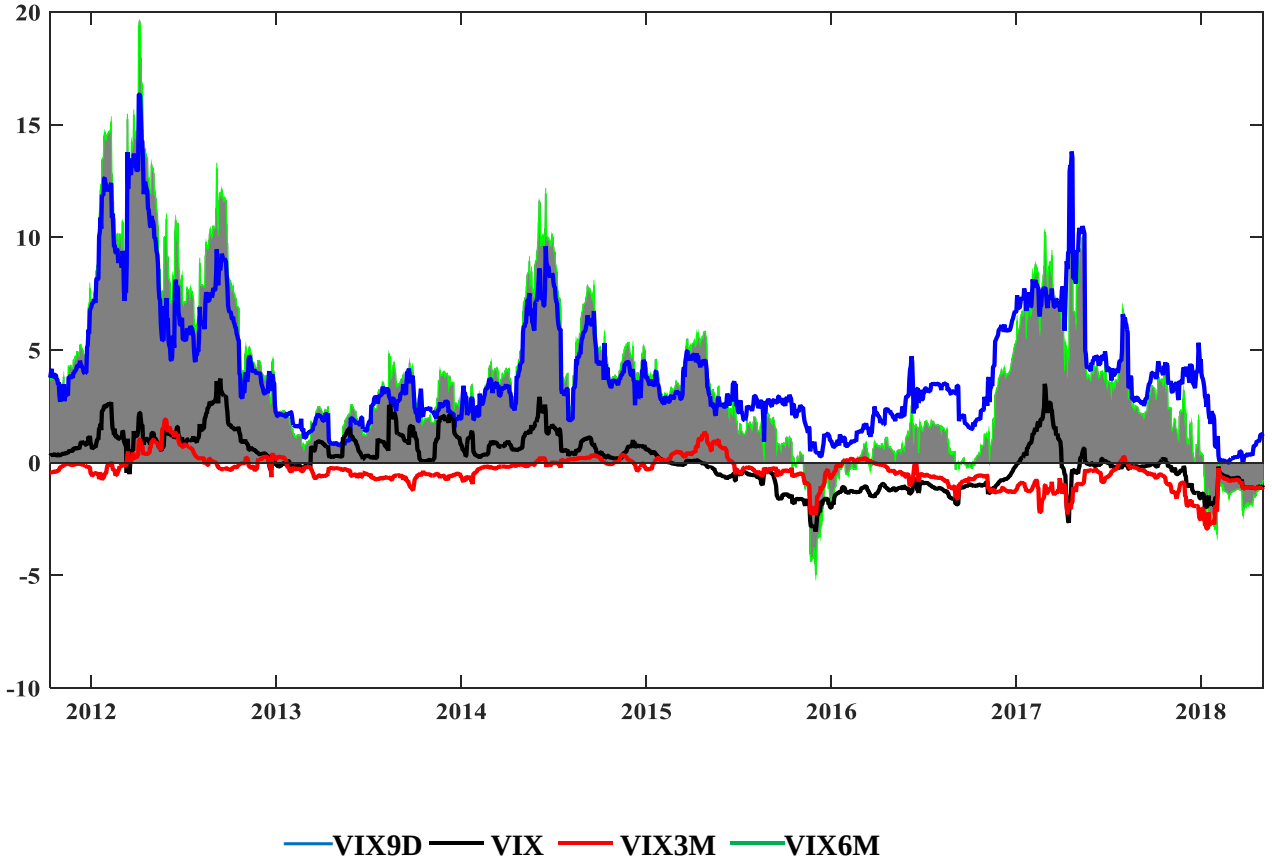

Figure 8: Generalized Impulse-Response Functions.

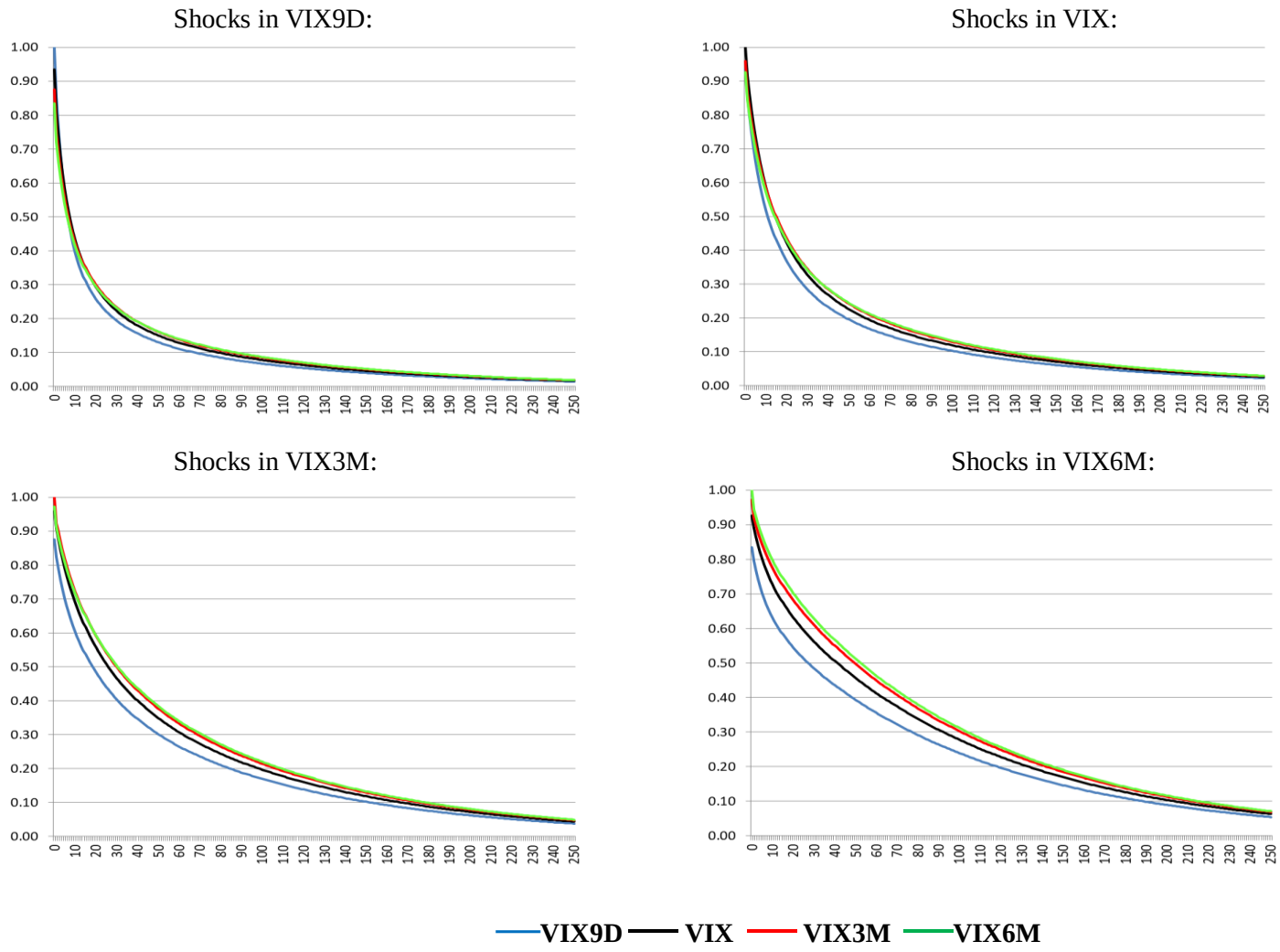

Figure 9: Total connectedness with TVP-VAR and Diebold-Yilmaz based on 200-day rolling windows.

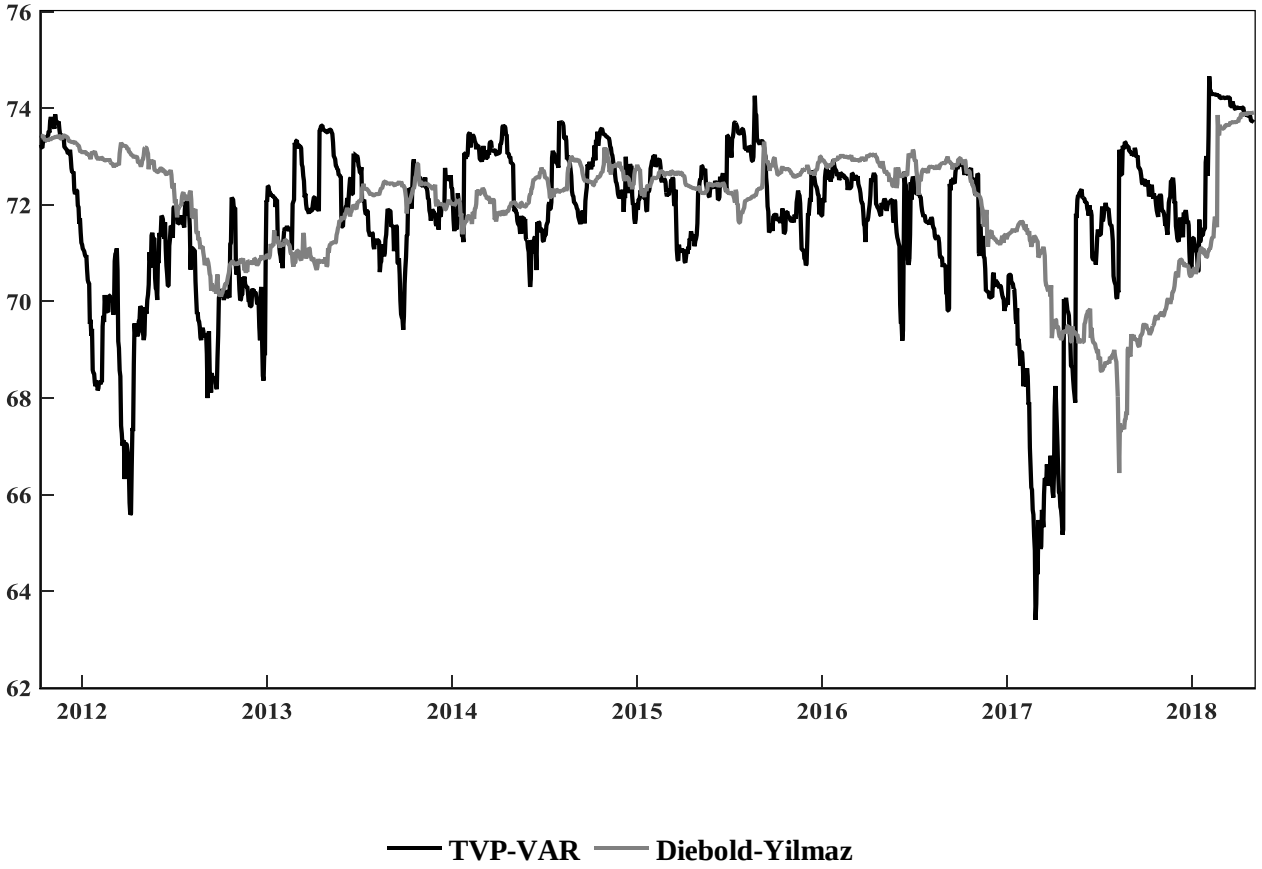

Note: Dynamic total connectedness of TVP-VAR with that of Diebold and Yilmaz (2012) with 200-day rolling windows. The sample period is from October 12, 2011 to May 4, 2018.

UB IREA
Institut de Recerca en Economia Aplicada Regional i Pública
Research Institute of Applied Economics
Universitat de Barcelona
Av. Diagonal, 690 • 08034 Barcelona

WEBSITE: www.ub.edu/irea/ • **CONTACT:** irea@ub.edu